# Size Effect of Cohesive Delamination Fracture Triggered by Sandwich Skin Wrinkling

**Zdeněk Bažant**
Northwestern University,
CEE, 2145 Sheridan Road,
Evanston, IL 60208

**Peter Grassl**[1]
University of Glasgow,
Glasgow, United Kingdom

*Because the observed size effect follows neither the strength theory nor the linear elastic fracture mechanics, the delamination fracture of laminate-foam sandwiches under uniform bending moment is treated by the cohesive crack model. Both two-dimensional geometrically nonlinear finite element analysis and one-dimensional representation of skin (or facesheet) as a beam on elastic-softening foundation are used. The use of the latter is made possible by realizing that the effective elastic foundation stiffness depends on the ratio of the critical wavelength of periodic skin wrinkles to the foam core thickness, and a simple description of the transition from shortwave to longwave wrinkling is obtained by asymptotic matching. Good agreement between both approaches is achieved. Skin imperfections (considered proportional to the the first eigenmode of wrinkling), are shown to lead to strong size dependence of the nominal strength. For large imperfections, the strength reduction due to size effect can reach 50%. Dents from impact, though not the same as imperfections, might be expected to cause as a similar size effect. Using proper dimensionless variables, numerical simulations of cohesive delamination fracture covering the entire practical range are performed. Their fitting, heeding the shortwave and longwave asymptotics, leads to an approximate imperfection-dependent size effect law of asymptotic matching type. Strong size effect on postpeak energy absorption, important for impact analysis, is also demonstrated. Finally, discrepancies among various existing formulas for critical stress at periodic elastic wrinkling are explained by their applicability to different special cases in the shortwave-longwave transition.*
[DOI: 10.1115/1.2722778]

Dedicated to Professor Franz Ziegler on the occasion of his 70th birthday

## 1 Introduction

A major question in extrapolating small-scale laboratory tests to full-scale sandwich structures is the size effect. Delamination of the skin (or facesheet) is often triggered by wrinkling instability, which has generally been considered to be free of size effect [1–5]. The absence of size effect has been inferred from the fact that the critical stress for buckling generally exhibits no size effect. However, this inference is valid only for the symmetry-breaking bifurcation of equilibrium path in perfect structures [6]. In actual sandwich structures, the geometrical shape of the skin is always geometrically imperfect, at least to some degree, due to imprecise manufacturing. Dents from impacts represent severe imperfections, usually accompanied by preexisting delaminations.

Buckling of imperfect quasibrittle structures generally leads to snapthrough instability which typically exhibits size effect on the nominal strength (e.g., [7] Chap. 13). The size effect is understood as the dependence of the dimensionless nominal strength of structure on its characteristic dimension (considered here as the skin thickness) when geometrically similar structures are compared (i.e., when all the structural dimensions are varied in proportion to the chosen characteristic dimension) [6,7]. The objective of this paper is to verify that this indeed happens for buckling driven delamination, to quantify the size effect, and to determine its intensity. A secondary objective is to assess the size effect on the postpeak energy absorption, important for judging survival under blast or dynamic impact.

Delamination in sandwiches and laminate composites has traditionally been analyzed by strength theory (either elastoplasticity or elasticity with strength limit) [8–14]. In this classical theory, there is no size effect.

Linear elastic fracture mechanics (LEFM) was applied to the analogous problem of delamination of micrometer-range metallic films from their substrate [15,16] and was also used in ([7], p. 770). For sandwich structures, however, LEFM now appears as unrealistic because, according to recent experiments [17,18], the size effect in typical laboratory tests is about half as strong as expected for LEFM. Therefore, the structure is quasibrittle [19], which means that the size of the fracture process zone (FPZ) cannot be considered to be negligible compared to the cross-sectional dimension of normal-size sandwich structures. Thus, delamination fracture should be simulated by the cohesive crack model rather than LEFM. This model has already been used in some recent numerical simulations [20,21] and will be adopted here.

Since buckling driven delamination is difficult to control in experiments, it is not surprising that only few experimental studies have been reported (e.g., [22,23]), and that none provides comprehensive insight. Thus, the present study will rely on numerical simulations using geometrically nonlinear finite element analysis as well as the softening foundation model, which is an adaptation of Winkler elastic foundation. Dimensionless variables will be used to cover the entire practical range. This goal will also necessitate clarifying confusion that still exists even for elastic skin wrinkling. It will be seen that different existing wrinkling formulas apply to different special cases, such a shortwave and longwave wrinkling.

This study deals exclusively with the deterministic size effect [6,7,24]. The Weibull-type statistical size effect on the mean struc-

[1]Formerly of Northwestern University, Evanston, IL.

Contributed by the Applied Mechanics Division of ASME for publication in the JOURNAL OF APPLIED MECHANICS. Manuscript received May 16, 2006; final manuscript received January 24, 2007. Review conducted by Robert M. McMeeking.

 Copyright © 2007 by ASME 

Downloaded 28 Nov 2007 to 129.105.215.213. Redistribution subject to ASME license or copyright; see http://www.asme.org/terms/Terms_Use.cfm

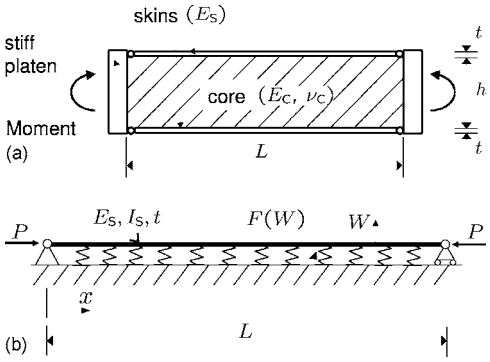


**Fig. 1 (*a*) The geometry of a typical sandwich beam subjected to pure bending and (*b*) the beam subjected to an axial compression force *P* supported by a softening foundation**

tural strength may, of course, also occur but must, in principle, be negligible when the location of failure initiation is fixed, either by mechanics or by defects, such as notches or dents. The present study is also limited to two-dimensional analysis of sandwich beams subjected to pure bending. Sandwich structures subjected to compression with or without bending are expected to lead to interaction of overall buckling and wrinkling (see Appendix), which is beyond the scope of this paper. So is the three-dimensional wrinkling, leading to two-dimensional delamination blisters, for which a similar, but probably weaker, size effects may be expected.

## 2 Softening Foundation Model

The analysis of delamination in sandwich structures subjected to pure bending, as shown in Fig. 1(*a*), can be simplified by modeling the skin as an axially compressed beam supported by a softening foundation consisting of independent continuously distributed nonlinear springs (Fig. 1(*b*)). For the mathematically analogous problem of a foundation with bilinear elastic-plastic hardening response, the solution is available [25]. Here, the problem is solved for bilinear elastic-softening response, in which the softening represents gradual decohesion due to a cohesive crack under the beam. The differential equation of the problem reads

$$E_s I_s \frac{d^4W}{dX^4} + P\frac{d^2W}{dX^2} + F = -P\frac{d^2W^\circ}{dX^2} \tag{1}$$

where $E_s$=Young's modulus of the skin, $I_s = t^3/12$=moment of inertia (per unit width) of the cross section of the skin of thickness $t$, $P$=axial force in the beam (per unit width), $X$=coordinate in the axial direction, and $W(X)$=deflection (lateral displacement) of the skin, additional to the initial deflection $W^\circ$. Furthermore, $F$ is the distributed lateral force (traction), defined as

$$F = \begin{cases} KW & \text{if } W \leqslant W_0 \\ KW_0 e^{-(W-W_0)/(W_f-W_0)} & \text{if } W > W_0 \end{cases} \tag{2}$$

where $K$ is the foundation modulus (i.e., the spring stiffness of the foundation per unit length), $W_0$ is the displacement at which the tensile strength $f_t$ is reached (Fig. 2) and $W_f$ controls the fracture energy $G_F$ of the cohesive crack, which lies in the core very near the skin,

$$G_F = f_t\left(W_f - \frac{W_0}{2}\right) \tag{3}$$

$G_F$ represents the total area under the stress-displacement curve in Fig. 2 (and not the area under the postpeak part of that curve, for unloading follows the elastic stiffness). The distributed spring stiffness $K$ (per unit length of beam) may be interpreted as

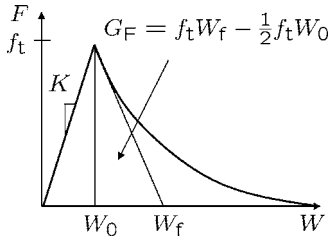


**Fig. 2 Force-displacement relation of the softening foundation**

$$K = \frac{E_c}{h_{eq}} \tag{4}$$

where $E_c$ is Young's modulus of the sandwich core and $h_{eq}$ represents the equivalent (or effective) depth of the foundation.

First, we consider the case of shortwave wrinkling of compressed skin, which is not affected by the opposite skin, and leave the case of interacting skins for later consideration. In this case, by contrast to many previous studies, $h_{eq}$ cannot be considered as constant. Rather, it depends on the stress field in the core below the skin (Fig. 3) and represents the thickness of a uniformly stressed strip of core material that gives the same foundation stiffness as the actual, nonuniformly stressed, core (and has a negligible shear modulus).

## 3 Elastic Shortwave Wrinkling and Equivalent Foundation Depth

Consider that the wavelength $L_{cr} \ll h$ ($h$=core thickness). In that case, and approximately if $L_{cr} < h$, the core may be regarded as an infinite half-space. The reason is that the alternating tractions applied on the core by the periodically wrinkled skin (Fig. 3(*b*)) are self-equilibrated over a segment of length $2L_{cr}$ where $L_{cr}$ is the half wavelength of skin buckling (Fig. 3(*c*)). Therefore, according to the St. Venant principle, the stresses caused by periodic wrinkling must exponentially decay to nearly zero over a distance from the skin roughly equal to $2L_{cr}$. Therefore, it must be possible to write

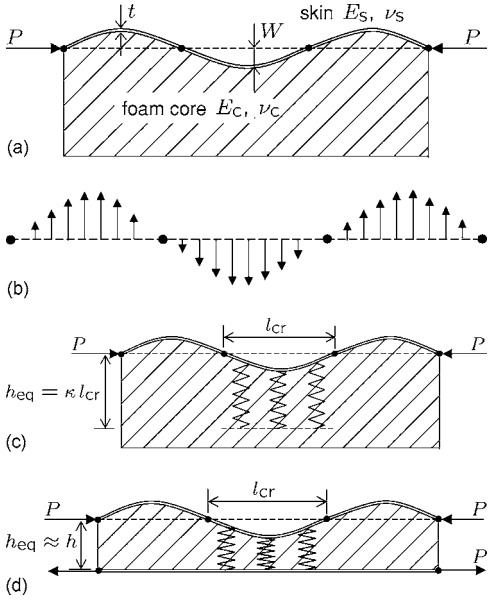


**Fig. 3 (*a*) The deflection of the top skin, (*b*) equilibriated stress acting on the foam, (*c*) equivalent height for shortwave, and (*d*) longwave wrinkling**



Downloaded 28 Nov 2007 to 129.105.215.213. Redistribution subject to ASME license or copyright; see http://www.asme.org/terms/Terms_Use.cfm

$$h_{eq_0} = \kappa L_{cr} \tag{5}$$

where $\kappa$ is some constant and subscript 0 refers to the limit case $L_{cr}/h \to 0$. For periodic skin buckling, the solution of the homogeneous differential equation for a beam on elastic foundation ([7], p. 316) yields

$$L_{cr} = \pi\left(\frac{E_s I_s}{K}\right)^{1/4} = \pi\left(\frac{\kappa L_{cr} E_s I_s}{E_c'}\right)^{1/4}, \quad I_s = \frac{t^3}{12} \tag{6}$$

where $I_s = t^3/12$ = central moment of inertia of the skin cross section (per unit width $b$). Solving (6) for $L_{cr}$ provides

$$L_{cr} = t\left(\frac{\pi^4 \kappa E_s}{12 E_c'}\right)^{1/3} \tag{7}$$

where $E_c'$ = effective Young's (elastic) modulus of the core; for plane stress, $E_c' = E_c$, and for plane strain, $E_c' = E_c/(1-\nu_c^2)$ where $\nu_c$ = Poisson ratio of the core. In this expression, $\nu_c$ accounts for the out-of-plane effect of Poisson ratio. Note that the in-plane effect of Poisson ratio, manifested in the effect of shear modulus $G_c = E_c'/2(1+\nu_c)$ of the core on its resistance to skin wrinkling, is known to be negligible in beam bending.

Thus, the critical axial compressive force in the skin at bifurcation is (per unit width $b$)

$$P_{cr_0} = 2\sqrt{K E_s I_s} = k_1 (E_c'^2 E_s)^{1/3} t \quad \text{where } k_1 = \left(\frac{2}{3\kappa^2 \pi^2}\right)^{1/3} \tag{8}$$

Note that this expression for $P_{cr}$ has the same form as that derived in [3] by solving the elastic boundary value problem problem under certain simplifications. The present derivation is far shorter, but it does not yield the value of $\kappa$. Comparison of the two expressions indicates dependence on $\nu_c$

$$\kappa = \alpha\sqrt{1+\nu_c} \tag{9}$$

The solution in [3] is matched if $\alpha = 0.43$. Here, however, $\alpha = 0.53$ is used, as determined from a single finite element analysis of $P_{cr}$.

A similar expression, namely, $P_{cr} = 0.85 t (E_s k_t^2)^{1/3}$ (where $k_t$ is a function of $E_c$), was proposed in [26] with $k_t$ taking into account the influence of orthotropic core.

## 4 Elastic Moment-Induced Longwave Wrinkling

Consider now that the critical wavelength $L_{cr} \gg h$ (Fig. 3($d$)) and that the sandwich beam is subjected to bending moment only (i.e., with no axial force). Then the opposite skin is under tension and may be approximated as a rigid base, with no deflection. The transverse compressive stress in the core is now almost uniform, and

$$h_{eq_\infty} = h \tag{10}$$

i.e., the foundation stiffness $K = E_c'/h_{eq}$ is constant (independent of the critical wavelength). The critical axial compressive force in the skin at bifurcation for periodic skin buckling (with no delamination) is ([7], p. 316)

$$P_{cr_\infty} = 2\sqrt{K E_s I_s} = \sqrt{\frac{E_c' E_s t^3}{3h}} \tag{11}$$

which is the same as reported in [4]; subscript $\infty$ refers to the limit case $L_{cr}/h \to \infty$, for which the solution is exact.

The hypothesis of the opposite skin being rigid is justified if the skin is sufficiently thick or subjected to sufficient tension, or both. Similar to shortwave wrinkling, the longwave wrinkling is resisted primarily by transverse normal stresses in the core, while the shear stresses in the core (which dominate global buckling) play a minor role.

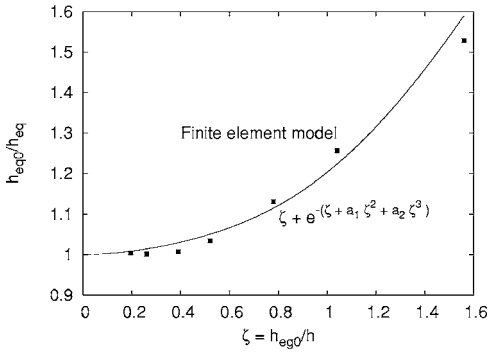


**Fig. 4 Evolution of the equivalent height $h_{eq}$ for the transition from shortwave to longwave wrinkling**

## 5 Asymptotic Matching of Elastic Shortwave-to-Longwave Transition

In general, the equivalent height $h_{eq}$ for both shortwave wrinkling in (5) and longwave wrinkling in (10) is subjected to the upper bound

$$h_{eq} = \min(h_{eq_0}, h_{eq_\infty}) \tag{12}$$

In reality, the transition between shortwave wrinkling and longwave wrinkling will not be abrupt but smoothly distributed over a certain range of the dimensionless variable

$$\zeta = \frac{h_{eq_0}}{h} \tag{13}$$

The shortwave bound $h_{eq} = h_{eq_0}$ must be tangentially approached for $\zeta \to 0$, and the longwave bound $h_{eq} = h_{eq_\infty}$ must be an asymptote for $\zeta \to \infty$. A smooth transition meeting these asymptotic conditions may simply be described by the function $h_{eq_0}/h_{eq} = \zeta + e^{-\zeta}$, which, however, has no free parameters to adjust according to finite element results. A more general expression that has such parameters, $a_1$ and $a_2$, and meets all the asymptotic conditions is

$$\frac{h_{eq_0}}{h_{eq}} = \zeta + e^{-(\zeta + a_1\zeta^2 + a_2\zeta^3)} \tag{14}$$

where $a_1 = 0.24$ and $a_2 = 0.36$, as obtained by fitting numerical results with the Marquardt-Levenberg algorithm for nonlinear least-squares optimization. The exponential decay in the expression for $h_{eq_0}/h_{eq}$ is favored by the fact that, according to St. Venant principle, the self-equilibrated tractions applied in a localized disturbance (such the wavelength of the skin) are known to decay with the distance from the disturbance exponentially. Comparisons of Eq. (14) to the results of finite element simulations are shown in Fig. 4.

Usually the end of a sandwich beam has either a laterally supported compressed skin or a zero bending moment (and thus no compression in the skin). In the rare case of an end with laterally sliding compressed skin ([7], p. 318) a semi-infinite skin wrinkles nonperiodically, as an exponentially decaying modulated sinusoid, and then both (8) and (11) must be divided by 2, with no change to the rest of analysis.

## 6 Formulation in Dimensionless Variables

The solution may generally be expressed as a relation among seven dimensional variables: $E_s I_s, K, P, W_0, W^\circ, W_f, x$ which involve two independent dimensions, force and length. According to the Vashy-Buckingham theorem of dimensional analysis, the number of dimensionless variables governing the problem is $7-2=5$. They may be chosen the same as in a previous study of plastic bilinearly hardening foundation [25]



Downloaded 28 Nov 2007 to 129.105.215.213. Redistribution subject to ASME license or copyright; see http://www.asme.org/terms/Terms_Use.cfm

$$x = X\left(\frac{E_s I_s}{K}\right)^{-1/4}, \quad \lambda = \frac{1}{2}P(KE_s I_s)^{-1/2} \tag{15}$$

$$w = \frac{W}{W_0}, \quad w^\circ = \frac{W^\circ}{W_0}, \quad w_f = \frac{W_f}{W_0} \tag{16}$$

Substituting Eqs. (15), (16), and (2) into (1), yields the dimensionless differential equation

$$\frac{d^4w}{dx^4} + 2\lambda\frac{d^2w}{dx^2} + w = -2\lambda\frac{d^2w^\circ}{dx^2} \quad \text{if } w \leqslant 1 \tag{17a}$$

$$\frac{d^4w}{dx^4} + 2\lambda\frac{d^2w}{dx^2} + e^{(w-1)/(w_f-1)} = -2\lambda\frac{d^2w^\circ}{dx^2} \quad \text{if } w > 1 \tag{17b}$$

where $w$=dimensionless deflection. For a perfect beam ($w^\circ=0$), the first eigenmode of buckling at bifurcation is determined from (17*a*) as $w=\sin x$, and the corresponding load at bifurcation results in $\lambda=1$.

A generic imperfection of skin may be expressed as a linear combination (or infinite series) of all the eigenmodes of elastic skin wrinkling. Similar to other buckling problems, the first eigenmode may be expected to have the dominant influence for loads near the first critical load [7]. Therefore, the imperfection $\delta$ of the skin is chosen to be proportional to the aforementioned displacement profile $w=\sin x$ of perfect skin at first bifurcation, i.e., $w^\circ = \delta \sin x$. The solution of (17) for the elastic case ($w_{\max} \leqslant 1$), with the aforementioned imperfection, is

$$w(x) = \frac{\lambda\delta}{1-\lambda}\sin x \tag{18}$$

This solution will be used in Sec. 9 for deriving the size effect law. The size effect is understood as the dependence of dimensionless nominal strength $\lambda$ on skin thin thickness $t$ when all the structural dimensions vary in proportion to $t$, i.e., $h/t$=const. For buckling failures with material failure criteria expressed solely in terms of stresses and strains, the size effect is nil [6], i.e., $\lambda$ is independent of $t$.

The dimensionless variables $x$, $w$, $w^\circ$, and $\lambda$ are size independent. However, ensuring constant fracture energy requires that the dimensionless parameter $w_f$ be considered size dependent, as obtained by inserting (3) into (16),

$$w_f = \frac{G_F E_c}{f_t^2 h_{eq}} + \frac{1}{2} \tag{19}$$

(note that this size dependence is analogous to the dependence of fracture energy on the mesh size in the crack band model [7,27]). Parameters $G_F$, $E_c$, and $f_t$ are material properties independent of the structure size, whereas $h_{eq}$ is proportional to the structure size. Thus, the size dependence of $w_f$ can be characterized as

$$w_f = \frac{1}{\xi} + \frac{1}{2} \tag{20}$$

where

$$\xi = \frac{h_{eq}}{l_0}, \quad l_0 = \frac{E_c G_F}{f_t^2} \tag{21}$$

$\xi$ is dimensionless and $l_0$ is known as Irwin's characteristic material length. For cracks in bulk, $l_0$ characterizes the fracture process zone length but not for delamination cracks (see [28,29] for opening and [30] for shear mode). What matters here is that $l_0$ represents a length parameter formed solely from basic material constants.

The initial boundary value problem solver of the commercial package MATLAB is used for numerical solution of the ordinary nonlinear differential equation (17). The amplitude of the initial displacement field is slightly increased in the middle of the beam, in order to control the location of the delamination growth. This increase is chosen to be so small that its effect on the magnitude of the load carried by the skin be imperceptible. The results are later compared to those of the finite element simulations in Sec. 8.

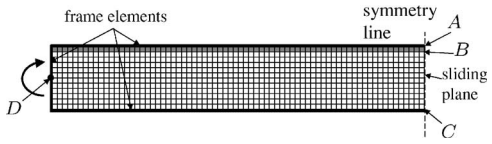


**Fig. 5 Finite element mesh**

To simplify analysis, only one half of the beam is modeled and symmetric deformation is assumed. Even though the actual growth of delamination blister must be expected to be nonsymmetric (one-sided) ([7], Chap. 12) the assumption of symmetry should be satisfactory because asymmetric growth of delamination fracture should produce a deflection curve symmetric with respect to a moving center of the blister.

When the delamination blister grows, the equivalent core depth below the blister (though not elsewhere) increases, which decreases the core stiffness. However, in view of satisfactory agreement with the finite element results, this effect appears to be minor and is not considered here.

## 7 Geometrically Nonlinear Finite Element Analysis

To determine parameter $\alpha$ in (17) and to validate the simplified modeling of delamination by the softening foundation model, a geometrically nonlinear finite element program (FEAP, procured from R. Taylor, Berkeley, CA) is used. A sandwich beam, depicted in Fig. 1(*a*), is considered and is modeled using the finite element mesh in Fig. 5. The skins are represented by beam elements taking into account large displacements and large rotations. For the core, plane stress finite elements based on a linearized small displacement formulation are used. The core is treated as isotropic, and for the skin, only the longitudinal elastic modulus $E_s$ needs to be considered since the transverse and shear moduli of laminate skin are immaterial for bending and axial deformation.

The beam is considered to be subjected to a uniform bending moment $M$. However, as long as the core thickness $h$ is large enough for the stresses from wrinkling to decay to nearly zero over the core thickness, the only loading that matters is the axial force in the skin, which is $P=M/(h+t)$. Whether this force is produced by moment alone, or a combination of bending moment and axial force, is immaterial.

An elastic stress-strain relation is used for all the elements of the core except a narrow band of elements under the skin (marked gray in Fig. 5). It is known that the delamination fracture occurs within the core very near the interface with the skin, but not within the interface. Therefore, perfect bond between the skins and the core is enforced. Transverse softening of the aforementioned band, which can be regarded as distributed microcracking, simulates delamination. In the softening band, the stress-strain law is elastic in the prepeak, and the postpeak response follows the isotropic damage model proposed in [27], which is defined as

$$\boldsymbol{\sigma} = (1-\omega)\mathbf{D}_c : \boldsymbol{\varepsilon} = (1-\omega)\bar{\boldsymbol{\sigma}} \tag{22}$$

Here, $\boldsymbol{\sigma}$ and $\boldsymbol{\varepsilon}$ are the stress and strain tensors in the core, $\bar{\boldsymbol{\sigma}}$ is the effective stress tensor, $\omega$ is the damage variable, and $\mathbf{D}_c$ is the isotropic elastic stiffness tensor of the core, which is based on the Young's modulus $E_c$ and the Poisson's ratio $\nu_c$. The damage variable $\omega$ is a function of history variable $\gamma$, which is defined as the maximum equivalent strain $\tilde{\varepsilon}$ reached in the history of the material: $\gamma(t)=\max \tilde{\varepsilon}(\tau)$ for $\tau \leqslant t$. The equivalent strain is defined as



Downloaded 28 Nov 2007 to 129.105.215.213. Redistribution subject to ASME license or copyright; see http://www.asme.org/terms/Terms_Use.cfm

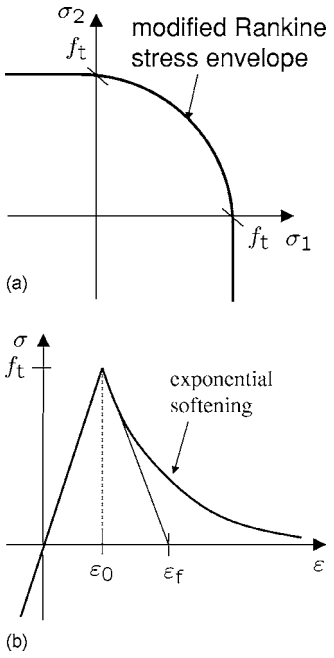


**Fig. 6 Initial stress envelope represented in the principal stress space obtained with the damage loading function**

$$\tilde{\varepsilon} = \frac{\sqrt{\langle \bar{\boldsymbol{\sigma}}_c \rangle : \langle \bar{\boldsymbol{\sigma}}_c \rangle}}{E_c} \tag{23}$$

where $\langle x \rangle = \max(x, 0)$. This definition corresponds to a Rankine-type strength envelope with a smooth round-off in the sectors of two positive principal stresses, as shown in Fig. 6(*a*).

The damage variable $\omega$ is related to the history variable $\gamma$ as

$$\omega = g(\gamma) = \begin{cases} 0 & \text{if } \gamma \leqslant \varepsilon_0 \\ 1 - \dfrac{\varepsilon_0}{\gamma} \exp\left( - \dfrac{\gamma - \varepsilon_0}{\varepsilon_f - \varepsilon_0} \right) & \text{if } \gamma \geqslant \varepsilon_0 \end{cases} \tag{24}$$

where $\varepsilon_0 = f_t / E_c$, $f_t$ is the tensile strength of the core. The parameter $\varepsilon_f$ is related to the fracture energy $G_F$ as

$$\varepsilon_f = \frac{G_F}{E_c \varepsilon_0 h_e} + \frac{1}{2} \varepsilon_0 \tag{25}$$

where $h_e$ is the depth of the element row (softening band) adjacent to the skin (Fig. 5). This damage law results in an exponential stress-strain curve in uniaxial tension, as presented in Fig. 6(*b*). The inelastic strains determined by the isotropic damage model are fully reversible, i.e., the secant stiffness points toward the origin (this reversibility would, of course, be unrealistic if crack unloading were not absent from the present simulations).

As before, only one-half of the beam is modeled (Fig. 5). The loading moment $M$ is applied at point $D$ and assumed to be transferred by a rigid loading platen into the upper and lower skins. The structure is restrained in longitudinal direction at point $A$. The loading is controlled by prescribing the displacement of point $B$. The same initial displacement, i.e., $w^{\circ} = \delta \sin x$, is prescribed for the upper skin. The imperfection amplitude $\delta$ at the middle of the beam at point $A$ is slightly increased in the same way as for the softening foundation model, to control the place where the delamination begins.

## 8 Results and Comparison of Softening Foundation to Finite Elements

The effect of the structure size on the relation between the load parameter $\lambda$ and the mid-point displacement $w_a = w(l/2)$ is shown,

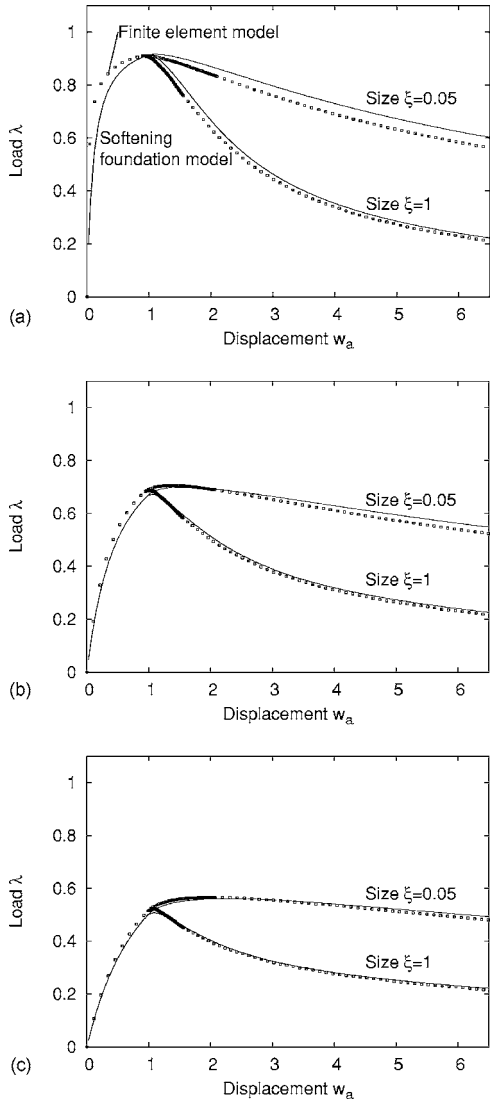


**Fig. 7 Load λ versus the midpoint displacement $w_a$ obtained with the softening foundation model and the finite element model for the imperfections: (*a*) $\delta$=0.1, (*b*) $\delta$=0.5, and (*c*) $\delta$=1 for two sizes ($\xi$=1 and $\xi$=0.05)**

for three imperfection amplitudes $\delta = 0.1, 1, 2$, in Fig. 7 (in which, $l = L(E_s I_s / K)^{-1/4}$, where the beam length $L$ is chosen to be $17 L_{cr}$.) As one can see, the results of the softening foundation model are in reasonable approximate agreement with the more accurate finite element results. The comparison shows that the size has a strong effect on the postpeak part of the load-displacement relation. The larger the size, the less energy is dissipated in relation to the energy dissipated by delaminating the entire skin. The deflection curves of the upper skins obtained from the softening foundation model for a constant imperfection $\delta$=0.1, and for the sizes $\xi$=1 and $\xi$=0.05, are shown in Fig. 8, respectively. In accordance with the load-displacement curves in Fig. 7, the lateral displacement $w_a$ for the small structure size is greater than for the large structure size. The overall deflection pattern is similar. However, a closer examination of the size effect on the evolution of the diagram of load versus blister length $b$ (which is the normalized length in the middle portion of the beam in which $w > 1$) reveals a size effect on the nominal strength; see Fig. 9. The larger the size, the smaller is $\lambda_{max}$ (i.e., it varies in proportion to the nominal strength, for the



Downloaded 28 Nov 2007 to 129.105.215.213. Redistribution subject to ASME license or copyright; see http://www.asme.org/terms/Terms_Use.cfm

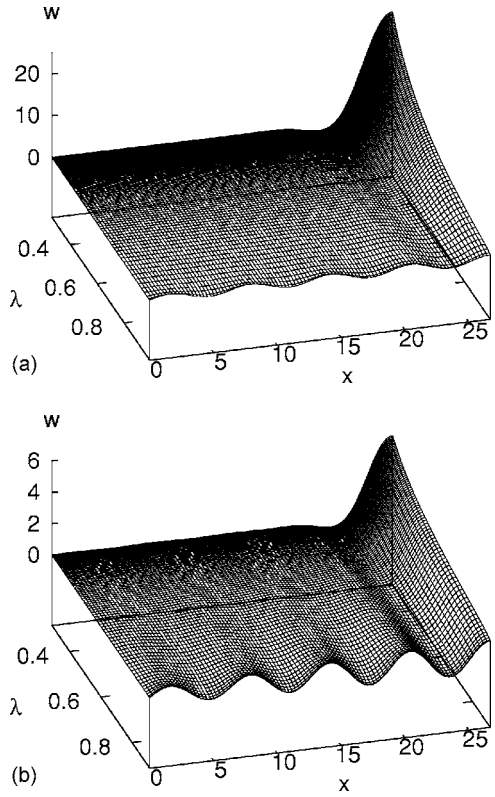


**Fig. 8 Deflection of the upper skin for the postpeak regime for imperfection $\delta$=0.1 and for the sizes: (*a*) $\xi$=0.05 and (*b*) $\xi$=1 obtained from the softening foundation model**

loading case presented in Fig. 1(*a*)). Furthermore, note that the size effect intensity depends strongly on the imperfection amplitude. A law for this size effect is proposed next.

## 9 Size Effect Law for Imperfection Sensitive Wrinkling

The size effect on the dimensionless nominal strength, $\lambda_N = \lambda_{\max}$, shown in Fig. 10, has a form similar to the size effect law for crack initiation in quasibrittle structures, which reads [6,19,24,31,32] $\lambda_N = \lambda_\infty[1+1/(k+\xi)]$, where $\lambda_\infty$ has the meaning of nominal strength of infinitely large structure. This law, however, is not directly applicable since imperfections are seen in Fig. 10 to influence the size effect. Therefore, a generalized law of the form

$$\lambda_N(\delta,\xi) = \lambda_\infty(\delta)\left[1 + \frac{1}{k(\delta) + a\xi^b}\right], \quad k(\delta) = c\delta^{-d} \tag{26}$$

is proposed here, with constants $a,b,c,d$ and parameters $\lambda_\infty$ and $k$, depending on the imperfection amplitude $\delta$. For large sizes ($\xi \to \infty$), the nominal strength is decided by initiation of cohesive crack ($w=1$), and in that case (18) leads to

$$\lambda_N(\delta,\infty) = \lambda_\infty = 1/(1+\delta) \tag{27}$$

Note that here the large-size limit does not correspond to LEFM, which is the case for type 2 size effect [24], seen in specimens with notches or large stress-free cracks. Rather, in the absence of preexisting delamination crack, we see a particular case of type 1 size effect [24] because the geometry is positive [6,19], causing failure to occur at crack initiation.

For small sizes ($\xi \to 0$), the nominal strength in (26) turns into

$$\lambda_N(\delta,0) = \lambda_\infty(\delta)\left[1 + \frac{1}{k(\delta)}\right] \tag{28}$$

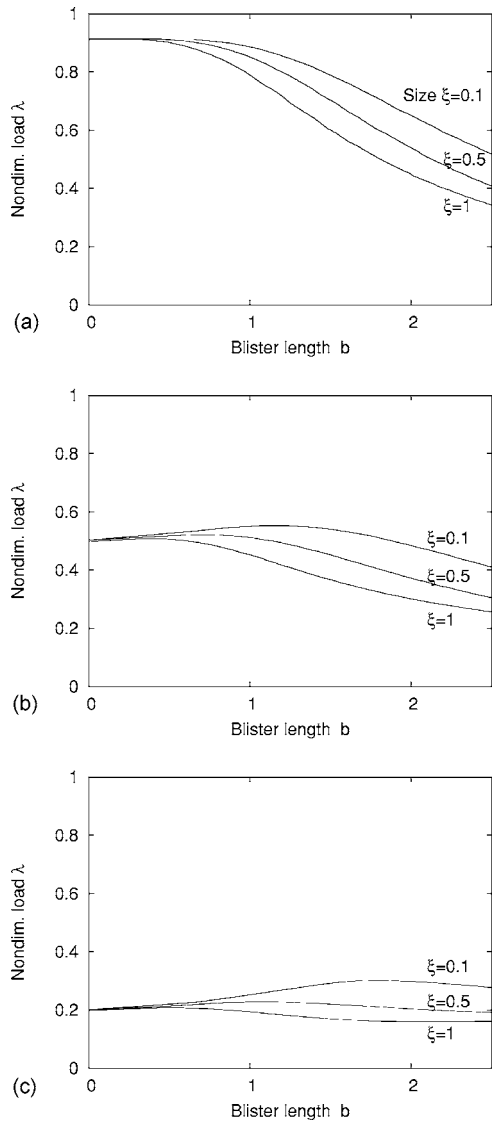


**Fig. 9 Load $\lambda$ versus the blister length (mid beam region in which $w>1$) of the upper skin for the imperfections: (*a*) $\delta$=0.1, (*b*) $\delta$=1, and (*c*) $\delta$=4 and for the sizes $\xi$=1, $\xi$=0.5, and $\xi$=0.1 obtained from the softening foundation model**

Parameters $a,b,c,d$ in (26) are determined as optimal fits of numerical results using the Marquardt-Levenberg algorithm for nonlinear least-squares optimization. First, the parameters $c$ and $d$ are determined from the fit of the results for the smallest size ($\xi$ =0.001) in Fig. 10, for varying imperfections. Then the parameters $a$ and $b$ in (26) are fitted for the largest imperfection ($\delta$ =6) and varying size. The optimum values are $a$=9.94, $b$=1.2, $c$=6.82, and $d$=1.21. The size effect law in (26) using these parameters is compared to the results of the softening foundation model in Fig. 10. The approximation is seen to be satisfactory.

To elucidate the typical values of $\xi$ and $\delta$ for small laboratory specimens, consider the material properties $E_c$=200 MPa, $\nu_c$ =0.25, $E_s$=150 GPa, $f_t$=1 MPa, $G_F$=750 N/m. Furthermore, let the skin thickness be $t$=0.001 m and let the beam height be so great that the assumption of shortwave wrinkling (Sec. 3) is valid. Equations (9), (7), and (5) give the equivalent height as $h_{eq}$ =0.0091 m. According to (21), the dimensionless size of the beam, is $\xi$=0.061. Furthermore, according to (16), the dimensionless amplitude $\delta$=6 corresponds to an imperfection amplitude of 27% of the skin thickness $t$. The nominal strength of this beam



Downloaded 28 Nov 2007 to 129.105.215.213. Redistribution subject to ASME license or copyright; see http://www.asme.org/terms/Terms_Use.cfm

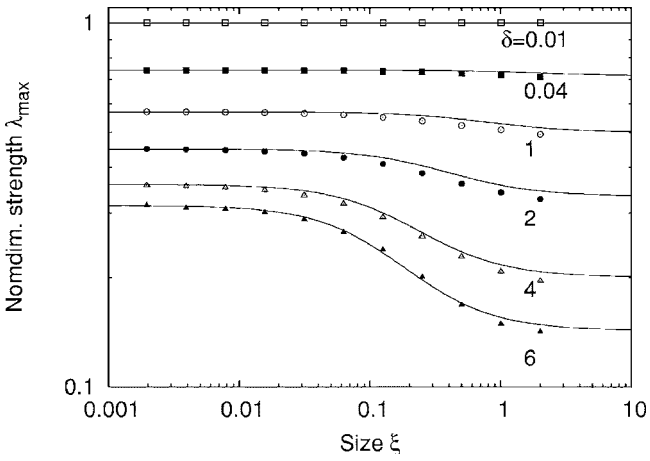


**Fig. 10 Comparison of the size effect law in Eq. (26) with the nominal strength-size curves obtained from the softening foundation model for different imperfections**

falls into the transitional range of the size effect law in Fig. 10. Therefore, up-scaling leads to a considerable reduction of the nominal strength.

## 10 Conclusions

1. In view of recent experiments revealing a size effect deviating from both LEFM and strength theory, the delamination fracture of laminate-foam sandwich structures must be treated as a cohesive crack with a softening stress-separation relation characterized by both fracture energy and tensile strength. In contrast to LEFM, no preexisting interface flaw needs to be considered.
2. The skin (or facesheet) can be treated as a beam on elastic-softening foundation, provided that the equivalent (or effective) core depth $h_{eq}$ for which the hypothesis of uniform transverse stress gives the correct foundation stiffness is considered to depend on the critical wavelength $L_{cr}$ of skin wrinkles; $h_{eq}$=core thickness $h$ for the asymptotic case of longwave wrinkling ($L_{cr}/h \to \infty$), while (because of St. Venant principle) $h_{eq} \propto L_{cr}$ for the asymptotic case of shortwave wrinkling ($L_{cr}/h \to 0$).
3. A properly formulated softening foundation model for the skin in sandwich beams subjected to bending moment can give good agreement with geometrically nonlinear finite element analysis of delamination fracture triggered by wrinkling.
4. Although the nominal strength of sandwich structures failing by wrinkling-induced delamination fracture is size independent when there is no imperfection, it becomes strongly size dependent with increasing imperfection. A size effect causing strength reduction by 50% is possible for larger imperfections. Dents from impact may be expected to have a similar effect, even though they are not merely geometrical imperfections (because of being usually accompanied by initial delamination).
5. Introduction of proper dimensionless variables makes it possible to cover with numerical simulations the entire practical range, and fitting the dimensionless numerical results for cohesive delamination fracture with a formula of correct shortwave and longwave asymptotics allows constructing an approximate size effect law for nominal strength of imperfect sandwich beams subjected to uniform bending moment.
6. There is also a strong size effect on postpeak energy absorption by a sandwich structure, both in the presence and absence of imperfections. This is important for impact and blast resistance.
7. The distinction between shortwave and longwave periodic wrinkling permits clarifying discrepancies among various existing formulas for elastic wrinkling, e.g., Hoff and Mautner's formula [3] applies to the limit of shortwave wrinkling, Heath's formula [4] to the limit of longwave wrinkling.

## Appendix: Comments on Transition to Global Buckling and "Naive" Optimization

The case where the opposite skins carry equal (or almost equal) axial force tends to produce skin wrinkling in which both skins deflect in the same direction. This is a different buckling mode—the global buckling of a sandwich beam in which the transverse normal stresses are negligible and the shear resistance of the core is paramount. The critical axial stress in the skins at bifurcation is given by Engesser's formula ([7], p. 32, 736)

$$\sigma_{cr_g} = \left(\frac{1}{2bt}\right)[F_{cr0}^{-1} + (Gbh)^{-1}]^{-1} \tag{A1}$$

Here, $G$=elastic shear modulus of the core, $F_{cr0}=(\pi^2/L_{ef}^2)R$ =Euler critical axial load corresponding to negligible shear deformation of the core, $L_{ef}$=effective buckling length of sandwich column, and $R$=bending stiffness $\approx b[t^3+3t(h+t)^2]E_s/6$ (note that Haringx's formula does not apply to sandwich buckling [33,34]).

A unified condition for bifurcation stress $\sigma$ in the skin, applicable to both skin wrinkling and global buckling (distinguished now by subscripts $w$ and $g$) may be written as $(\sigma-\sigma_w)(\sigma-\sigma_g)=0$, where $\sigma_w$, $\sigma_g$=maximum stresses for wrinkling of imperfect skin or buckling of imperfect column, each considered alone. However, according to Koiter ([7], Sec. 4.6) proximity of two critical loads generally enhances imperfection sensitivity. Thus, when $\sigma_w$ and $\sigma_g$ are nearly equal, the maximum stress $\sigma$ for combined wrinkling and buckling gets reduced. This could be approximately captured by the following relation:

$$(\sigma - \sigma_w{}^p)(\sigma - \sigma_g{}^r) = r^{p+q} \tag{A2}$$

where $p, q$ are positive empirical constants (probably of the order of 1) and $r$ is a measure of failure stress reduction due to mode interaction. If one term of the product in this equation tends to $\infty$, the other must tend to 0, i.e., the equation implies the individual critical stresses $\sigma_w$ and $\sigma_g$. Equation (A2) also has the necessary property that the reduction of failure stress $\sigma$ is maximum when the two critical stresses coincide. These features agree with the well-known fact that the so-called naive optimum designs, in which one or more critical stresses coincide, ought to be avoided. However, verification, calibration or possible modification of Eq. (A2) is beyond the scope of this study.

## References


[1] Reissner, M. E., 1937, "On the Theory of Beams Resting on a Yielding Foundation," Proc. Natl. Acad. Sci. U.S.A., **23**, pp. 328–333.
[2] Gough, G. S., Elam, C. F., and de Bruyne, N. A., 1940, "The Stabilisation of a Thin Sheet by a Continuous Supporting Medium," J. R. Aeronaut. Soc., **44**, pp. 12–43.
[3] Hoff, N. J., and Mautner, S. E., 1945, "The Buckling of Sandwich-Type Panels," J. Aeronaut. Sci., **12**, pp. 285–297.
[4] Heath, W. G., 1960, "Sandwich Construction, Part 2: The Optimum Design of Flat Sandwich Panels," Aircr. Eng., **32**, pp. 230–235.
[5] Niu, K., and Talreja, R., 1999, "Modeling of Wrinkling in Sandwich Panels Under Compression," J. Eng. Mech., **125**(8), pp. 875–883.
[6] Bažant, Z. P., 2002, *Scaling of Structural Strength*, Hermes-Penton, London (and 2nd ed., Elsevier, New York, 2005).
[7] Bažant, Z. P., and Cedolin, L., 1991, *Stability of Structures: Elastic, Inelastic, Fracture and Damage Theories*, Oxford University Press, London.
[8] Sallam, S., and Simitses, G. J., 1985, "Delamination Buckling and Growth of Flat, Cross-Ply Laminates," Compos. Struct., **4**, pp. 361–381.
[9] Yin, W. L., Sallam, S., and Simitses, G. J., 1986, "Ultimate Axial Load Capacity of a Delaminated Beam-Plate," AIAA J., **34**, pp. 123–128.
[10] Daniel, I. M., and Ishai, O., 1994, *Engineering Mechanics of Composite Materials*, Oxford University Press, New York.
[11] Wadee, M. A., and Blackmore, A., 2001, "Delamination From Localized Instabilities in Compression Sandwich Panels," J. Mech. Phys. Solids, **49**, pp. 1281–1299.




Downloaded 28 Nov 2007 to 129.105.215.213. Redistribution subject to ASME license or copyright; see http://www.asme.org/terms/Terms_Use.cfm

[12] Wadee, M. A., 2002, "Localized Buckling in Sandwich Struts With Pre-Existing Delaminations and Geometrical Imperfections," J. Mech. Phys. Solids, **50**, pp. 1767–1787.
[13] Frostig, Y., and Thomsen, O. T., 2005, "Non-Linear Behavior of Delamination Unidirectional Sandwich Panels With Partial Contact and a Transversely Flexible Core," Int. J. Non-Linear Mech., **40**, pp. 633–651.
[14] Aviles, F., and Carlsson, L. A., 2005, "Elastic Foundation Analysis of Local Face Buckling in Debonded Sandwich Columns," Mech. Mater., **37**, pp. 1026–1034.
[15] Hutchinson, J. W., and Suo, Z., 1992, "Mixed Mode Cracking in Layered Materials," Adv. Appl. Mech., **29**, pp. 63–191.
[16] Jensen, H. M., and Sheinman, I., 2002, "Numerical Analysis of Buckling-Driven Delamination," Int. J. Solids Struct., **39**, pp. 3373–3386.
[17] Bažant, Z. P., Zhou, Y., and Daniel, I. M., 2006, "Size Effect on Strength of Laminate-Foam Sandwich Plates," ASME J. Eng. Mater. Technol., **128**, pp. 366–374.
[18] Bayldon, J., Bažant, Z. P., Daniel, I. M., and Yu, Q., 2006, "Size Effect on Compressive Strength of Laminate-Foam Sandwich Plates," ASME J. Eng. Mater. Technol., **128**, pp. 169–174.
[19] Bažant, Z. P., and Planas, J., 1998, *Fracture and Size Effect in Concrete and Other Quasibrittle Materials*, CRC Press, Boca Raton.
[20] Remmers, J. J. C., and de Borst, R., 2001, "Delamination Buckling of Fibre-Metal Laminates," Compos. Sci. Technol., **61**, pp. 2207–2213.
[21] Han, T., Ural, A., Chen, C., Zehnder, A. T., Ingraffea, A. R., and Billington, S. L., 2002, "Delamination Buckling and Propagation Analysis of Honeycomb Panels Using a Cohesive Element Approach," Int. J. Fract., **115**, pp. 101–123.
[22] Gdoutos, E. E., Daniel, I. M., and Wang, K.-A., 2003, "Compression Facing Wrinkling of Composite Sandwich Structures," Mech. Mater., **35**, pp. 511–522.
[23] Vadakke, V., and Carlsson, L. A., 2004, "Experimental Investigation of Compression Failure of Sandwich Speciments With Face/Core Debond," Composites, Part B, **35**, pp. 583–590.
[24] Bažant, Z. P., 2004, "Scaling Theory for Quasibrittle Structural Failure," Proc. Natl. Acad. Sci. U.S.A., **101**, pp. 13400–13407.
[25] Tvergaard, V., and Needleman, A., 1980, "On the Localization of Buckling Patterns," ASME J. Appl. Mech., **47**, pp. 613–619.
[26] Vonach, W. K., and Rammerstorfer, F. G., 2000, "The Effects of In-Plane Core Stiffness on the Wrinkling Behavior of Thick Sandwiches," Acta Mater., **141**, pp. 1–10.
[27] Bažant, Z. P., and Oh, B.-H., 1983, "Crack Band Theory for Fracture of Concrete," Mater. Struct., **16**, pp. 155–177.
[28] Suo, Z., Bao, G., and Fan, B., 1992, "Delamination R-Curve Phenomena Due to Damage," J. Mech. Phys. Solids, **40**, pp. 1–16.
[29] Bao, G., and Suo, Z., 1992, "Remarks on Crack-Bridging Concepts," Appl. Mech. Rev., **45**, pp. 355–366.
[30] Massabó, R., and Cox, B. N., 1999, "Concepts for Bridged Mode II Delamination Cracks," J. Mech. Phys. Solids, **47**(6), pp. 1265–1300.
[31] Bažant, Z. P., and Yavari, A., 2004, "Is the Cause of Size Effect on Structural Strength Fractal or Energetic-Stastical," Eng. Fract. Mech., **72**, pp. 1–31.
[32] Bažant, Z. P., 1997, "Scaling of Quasi-Brittle Fracture: Asymptotic Analysis," Int. J. Fract., **83**, pp. 19–40.
[33] Bažant, Z. P., and Beghini, A., 2005, "Which Formulation Allows Using a Constant Shear Modulus for Small-Strain Buckling of Soft-Core Sandwich Structures," ASME J. Appl. Mech., **72**, pp. 785–787.
[34] Bažant, Z. P., and Beghini, A., 2006, "Stability and Finite Strain of Homogenized Structures Soft in Shear: Sandwich or Fiber Composites, and Layered Bodies," Int. J. Solids Struct., **43**, pp. 1571–1593.



**Downloaded 28 Nov 2007 to 129.105.215.213. Redistribution subject to ASME license or copyright; see http://www.asme.org/terms/Terms_Use.cfm**